

13146

Planets as Background Noise Sources in Free Space Optical Communications

J. Katz

Advanced Electronic Materials and Devices Section

Background noise generated by planets is the dominant noise source in most deep space direct detection optical communications systems. Earlier approximate analyses of this problem are based on simplified blackbody calculations and can yield results that may be inaccurate by up to an order of magnitude. This article points out various other factors that need to be taken into consideration, such as the phase angle and the actual spectral dependence of the planet albedo, in order to obtain a more accurate estimate of the noise magnitude.

I. Introduction

Optical communications is considered as an alternative to conventional microwave links in future planetary (and exosolar) space missions (Ref. 1). For many typical deep space communications scenarios, the optical receiver which achieves maximum link sensitivity employs direct detection with a photon counting detector (e.g., photomultiplier tube) at the front end (Ref. 2). The performance of such receivers is limited by either the photon statistics of the received signal light or by background noise photons that appear in the receiving telescope field of view. In planetary space missions, the dominant background noise sources are the planets. Not only are they the brightest objects in the solar system (except the sun), but the highest demand on the communication link usually occurs during the planetary fly-by phase, where they are almost certain to be in the receiver field of view.

A first order approximation to the planet background noise is based on simplified blackbody calculations (for the spectral dependence), including the planet albedo as a single unique parameter (Refs. 3, 4, 5). As will be discussed in the following sections, the problem is much more involved, and the actual result can vary by more than an order of magnitude as compared to this simplified calculation. The purpose of this

article is to point out the other parameters that need to be taken into account and to demonstrate their effect through some illustrative examples. This article is not meant to be an exhaustive study of the problem. Such a detailed analysis is relevant only in the context of an actual planned mission.

Section II will briefly review the approximate basic theory. The following sections will consider the effects of the planet being an extended or a point source (Section III), phase angle (Section IV), and spectral dependence (Section V). Two other effects (polarization and temporal variations) will be briefly mentioned in Section VI.

II. Basic Theory

For the visible and near-infrared regions of the spectrum, virtually all the planet radiation is from reflected sunlight. The situation is different in the mid and far infrared (Ref. 3), but these cases will not be considered here.

If the planet is replaced by an ideal lambertian disk with a unit reflectivity facing the sun and with the same radius as the planet, the irradiance at the receiver plane is:

$$E_{\lambda} = \frac{H_{\lambda}}{R_{P_{\odot}}^2} \left(\frac{R_p}{Z} \right)^2 \frac{W}{\text{cm}^2 \mu\text{m}} \quad (1)$$

where H_{λ} is the solar flux at 1 AU (see Fig. 1 and Table 1), $R_{P_{\odot}}$ is the sun-planet distance in AU, R_p is the planet radius (in km), and Z is the distance between the planet and the receiver — usually earth — in km. Since the planets' orbits are not circular, there will be some variations due to the orbit eccentricity. The magnitude of this effect, with other basic parameters of the planets, are listed in Table 2. The ratio between the actual irradiance to the one predicted by Eq. (1) is the geometric albedo, p , of the planet.

By multiplying the actual irradiance by the receiver aperture area and by the bandwidth of its optical filter we obtain the background power level at the detector.

The simplified worst case calculations are given in Refs. 3, 4, and 5 (it should be noted that there is error in those references where the curves corresponding to Mars and Mercury are interchanged), where a single number is used to represent the albedo of each planet. In the following sections we will consider the various factors affecting the geometric albedo.

III. Planets as Extended Sources or Point Sources

Planetary optical communication receivers are usually envisioned to have narrow fields of view, usually in the micro-radian regime. Thus in many cases where the angular extent of the planet, θ_p , exceeds the receiver field of view, θ_r , the planet appears as an extended background source. Table 3 lists the approximate minimum, maximum and typical values of θ_p of each planet for near-earth reception. For uniformly reflecting planets the background irradiance dependence on θ_r is as shown in Fig. 2. Some planets, though, do not reflect uniformly, as shown, for example, for the planet Mars in Fig. 3, and thus when $\theta_r < \theta_p$, planetary features may have to be considered in greater detail. Of course, when $\theta_r > \theta_p$ (i.e., the planet is entirely encompassed by the receiver field of view) all the planet spatial features are averaged out.

IV. Phase-Angle Dependence

The phase angle is defined as the sun-planet-receiver (earth) angle. Even if the geometric albedo did not depend on the phase angle, the background contribution from the planet will vary because at the various phases different portions of the illuminated planet are seen from earth. This effect, which is

most important for the inner planets (and the moon), is analyzed in more detail in Appendix A and is depicted in Fig. 4.

In addition, there is a basic dependence of the geometric albedo on the phase angle α , because planets are not ideal lambertian reflectors. This dependence is expressed by a phase function $\phi(\alpha)$, which is shown in Fig. 5 for the planet Mars (Ref. 8) and the moon (Ref. 9). The typical features of the phase function are a linear part for phase angles exceeding approximately 10 deg, and a higher order component for phase angles smaller than approximately 5 deg. This enhanced reflectivity at small phase angles is called the "opposition effect." The exact shape of the phase function depends on the detailed light scattering properties at the planet (Refs. 8 and 9). Generally, albedos of planets with atmospheres have a smaller dependence on the phase angle than atmosphereless planets.

V. Spectral Dependence

In many cases the geometric albedo depends strongly on the wavelength. This may be caused, for example, by absorption lines in the planet's atmosphere or other processes such as Raman Scattering. Examples of the spectral variations of the albedo are shown in Fig. 3 (for Mars), Fig. 6 (for several planets in general low resolution detail) and in Fig. 7 for some other planets in more detail (Venus, Jupiter, Uranus, and Neptune). It is clearly seen that with all other parameters equal, a judicious choice of the communications link wavelength can significantly reduce the background noise by even more than an order of magnitude. For example, the Mars albedo at $\lambda = 1 \mu\text{m}$ is three to four times larger than at $\lambda = 0.5 \mu\text{m}$ (this is somewhat offset by the fact that the photon irradiance of the sun is 1.5 times larger at $0.5 \mu\text{m}$ than at $1 \mu\text{m}$). Furthermore, other outer planets which have atmospheres appear very dark at several wavelength regions, and they will contribute negligibly low background noise levels if these wavelengths are utilized in the communication link.

VI. Other Factors

In addition to the parameters discussed in the earlier sections, there are other factors that are usually of secondary importance, and are mentioned here for the sake of completeness. The first is the fact that planets — like most other objects — do not reflect equally both light polarizations. This effect is small (see data for Venus and Earth in Fig. 8) and completely unimportant in systems using unpolarized light or light with unknown polarization. The second factor is various temporal variations that can be caused by planetary climate patterns, solar flares, and other phenomena. Again, these are minor

effects compared with the effects of the Earth-Planet distance variation, phase angle and spectral dependence discussed earlier.

VII. Conclusion

As shown in the earlier sections, the simplified calculations of background noise generated by planets (Refs. 3, 4, 5) pre-

dict worst case situations and can thus serve in many cases only as a first order approximation to the actual magnitude of the background. While exact results can be obtained only when all the mission parameters are known (e.g., Planet and Earth location with respect to the Sun), this article points out the various parameters that play a role in determining this final result. The most important conclusion is that the noise magnitude strongly depends on the wavelength used for communication.

Acknowledgment

Discussions with S. Dolinar were helpful in ascertaining the dependence of received background noise from Venus on the Earth-Sun-Venus angle.

References

1. Posner, E. C., Grant, T., and Hortor, R., "Communications and Navigation for Galileo and Future Outer Planets Spacecraft," *IEEE Spectrum* (to be published), June 1986.
2. Lesh, J. R., Katz, J., Tan, H. H., and Zwillinger, D., "2.5 Bit/Detected Photon Demonstration Program: Description, Analysis, and Phase I Results," *TDA Progress Report 42-66*, Jet Propulsion Laboratory, Pasadena, Calif., pp. 115-132, 1981.
3. Ramsey, R. C., "Spectral Irradiance from Stars and Planets, above the Atmosphere, from 0.1 to 100.0 Microns," *Appl. Opt. 1*, 465-471, 1962.
4. Katz, J., "The Deep-Space Optical Channel: I. Noise Mechanisms," *TDA Progress Report 42-64*, Jet Propulsion Laboratory, Pasadena, Calif., 180-186, 1981.
5. Vilnrotter, V. A., "Background Sources in Optical Communications," *JPL Publication 82-73*, Jet Propulsion Laboratory, Pasadena, Calif., 1983.
6. "Solar Electromagnetic Radiation," NASA SP-8005, Washington, D.C., 1971.
7. "Surface Models of Mars (1975)," NASA SP-8020, Washington, D.C., 1975.
8. Egan, W. G., *Photometry and Polarization in Remote Sensing*, New York: Elsevier, 1985.
9. Lumme, K., and Bowell, E., "Radiative Transfer in the Surfaces of Atmosphereless Bodies," *Astron. J.* "I. Theory," 86 1694-1704, 1981; "II. Interpretation of Phase Curves," 86, 1705-1771, 1981; "III. Interpretation of Lunar Photometry," 87, 1076-1082, 1982.
10. Hartmann, W. K., *Moons and Planets: An Introduction to Planetary Science*, Tarrytown-on-Hudson, New York: Bogden and Quigley, 1972.
11. Moroz, V. I., "Stellar Magnitude and Albedo Data of Venus" (Ch. 3) in *Venus*, D. M. Hunten et al., Eds. Tucson: The U. of Arizona Press, 1983.
12. Taylor, D. J., "Spectrophotometry of Jupiter's 34100-1000Å Spectrum and a Bolometric Albedo for Jupiter," *Icarus*, 4, 362-373, 1965.
13. Irvine, W. M., and Lane, A. P., "Monochromatic Albedos for the Disk of Saturn," *Icarus*, 15, 18-26, 1971.
14. Neff, J. S., et al., "Absolute Spectrophotometry of Titan, Uranus and Neptune: 3500-10,500Å," *Icarus*, 60, 221-235, 1984.
15. Coffeen, D. L., and Hansen, J. E., "Polarization Studies of Planetary Atmospheres," from *Planets, Stars and Nebulae, Studied with Photopolarimetry*, T. Gehrels, Ed. Tucson: The U. of Arizona Press, 1974.

Table I. Solar spectral irradiance at 1 AU (from Ref. 6)

Wavelength (λ), μm	Average Irradiance* (P_λ), $\text{W cm}^{-2} \mu\text{m}^{-1}$	Wavelength (λ), μm	Average Irradiance* (P_λ), $\text{W cm}^{-2} \mu\text{m}^{-1}$	Wavelength (λ), μm	Average Irradiance* (P_λ), $\text{W cm}^{-2} \mu\text{m}^{-1}$
0.120	0.000010	0.425	0.1693	0.740	0.1260
0.140	0.000003	0.430	0.1639	0.750	0.1235
0.150	0.000007	0.435	0.1663	0.800	0.1107
0.160	0.000023	0.440	0.1810	0.850	0.0988
0.170	0.000063	0.445	0.1922	0.900	0.0889
0.180	0.000125	0.450	0.2006	0.950	0.0835
0.190	0.000271	0.455	0.2057	1.000	0.0746
0.200	0.00107	0.460	0.2066	1.100	0.0592
0.210	0.00229	0.465	0.2048	1.200	0.0484
0.220	0.00575	0.470	0.2033	1.300	0.0396
0.225	0.00649	0.475	0.2044	1.400	0.0336
0.230	0.00667	0.480	0.2074	1.500	0.0287
0.235	0.00593	0.485	0.1976	1.600	0.0244
0.240	0.00630	0.490	0.1950	1.700	0.0202
0.245	0.00723	0.495	0.1960	1.800	0.0159
0.250	0.00704	0.500	0.1942	1.900	0.0126
0.255	0.0104	0.505	0.1920	2.000	0.0103
0.260	0.0130	0.510	0.1882	2.100	0.0090
0.265	0.0185	0.515	0.1833	2.200	0.0079
0.270	0.0232	0.520	0.1833	2.300	0.0068
0.275	0.0204	0.525	0.1852	2.400	0.0064
0.280	0.0222	0.530	0.1842	2.500	0.0054
0.285	0.0315	0.535	0.1818	2.600	0.0048
0.290	0.0482	0.540	0.1783	2.700	0.0043
0.295	0.0584	0.545	0.1754	2.800	0.00390
0.300	0.0514	0.550	0.1725	2.900	0.00350
0.305	0.0603	0.555	0.1720	3.000	0.00310
0.310	0.0689	0.560	0.1695	3.100	0.00260
0.315	0.0764	0.565	0.1705	3.200	0.00226
0.320	0.0830	0.570	0.1712	3.300	0.00192
0.325	0.0975	0.575	0.1719	3.400	0.00166
0.330	0.1059	0.580	0.1715	3.500	0.00146
0.335	0.1081	0.585	0.1712	3.600	0.00135
0.340	0.1074	0.590	0.1700	3.700	0.00123
0.345	0.1069	0.595	0.1682	3.800	0.00111
0.350	0.1093	0.600	0.1666	3.900	0.00103
0.355	0.1083	0.605	0.1647	4.000	0.00095
0.360	0.1068	0.610	0.1635	4.100	0.00087
0.365	0.1132	0.620	0.1602	4.200	0.00078
0.370	0.1181	0.630	0.1570	4.300	0.00071
0.375	0.1157	0.640	0.1544	4.400	0.00065
0.380	0.1120	0.650	0.1511	4.500	0.00059
0.385	0.1098	0.660	0.1486	4.600	0.00053
0.390	0.1098	0.670	0.1456	4.700	0.00048
0.395	0.1189	0.680	0.1427	4.800	0.00045
0.400	0.1429	0.690	0.1402	4.900	0.00041
0.405	0.1644	0.700	0.1369	5.000	0.0003830
0.410	0.1751	0.710	0.1344	6.000	0.0001750
0.415	0.1774	0.720	0.1314	7.000	0.0000990
0.420	0.1747	0.730	0.1290	8.000	0.0000600

*Special irradiance averaged over small bandwidth centered at λ : 0.3 to 0.75 μm (bandwidth, 100Å), 0.75 to 1.0 μm (bandwidth, 500Å), and 1.0 to 5.0 μm (bandwidth, 1000Å)

Table 2. Orbital constants of the planets and solar irradiance at planetary distances (from Ref. 6)

Planet	Semi-Major Axis of Orbit		Sidereal Period, days	Eccentricity of Orbit 1971, ϵ	Solar Irradiance at Distance of Semi-Major Axis*		Ratio of Max to Min Irradiance,** $\left(\frac{1+\epsilon}{1-\epsilon}\right)^2$
	AU	10^6 km			Solar Constant	mW cm^{-2}	
Mercury	0.387 099	57.91	87.9686	0.205 629	6.673 5	902.9	2.303
Venus	0.723 332	108.21	224.700	0.006 787	1.911 3	258.6	1.028
Earth	1.000	149.60	365.257	0.016 721	1.000 0	135.3	1.069
Mars	1.523 69	227.94	686.980	0.093 379	0.430 7	58.28	1.454
Jupiter	5.2028	778.3	4 332.587	0.048 122	0.036 95	4.999	1.212
Saturn	9.540	1427	10 759.20	0.052 919	0.010 99	1.487	1.236
Uranus	19.18	2869	30 685	0.049 363	0.002 718	0.3678	1.218
Neptune	30.07	4498	60 188	0.004 362	0.001 106	0.1496	1.018
Pluto	39.44	5900	90 700	0.252 330	0.000 643	0.0870	2.806

*Solar irradiance is $1/R^2$ in units of the solar constant and $135.3/R^2$ in mW cm^{-2} where R is the semi-major axis of the planetary orbit.
 **Values of eccentricity change with time; the ratio of solar irradiance at perihelion to that at aphelion in the last column is computed on the assumption of constant eccentricity.

Table 3. Approximate angles (in microradians) subtended by planets ¹

Planet	Minimum ²	Maximum ³	Typical ⁴
Mercury	23	53	33
Venus	47	292	81
Mars	18	87	30
Jupiter	153	225	182
Saturn	76	94	84
Uranus	19	17	18
Neptune	6	6	6
Pluto	2	2	2

¹ Does not include the partially lit area effect which is primarily important for the inner planets as discussed in Appendix A.
² At maximum Earth-Planet distance.
³ At minimum Earth-Planet distance.
⁴ Earth-Planet distance equals 1 AU for the inner planets and Sun-Planet distance of the outer planets.

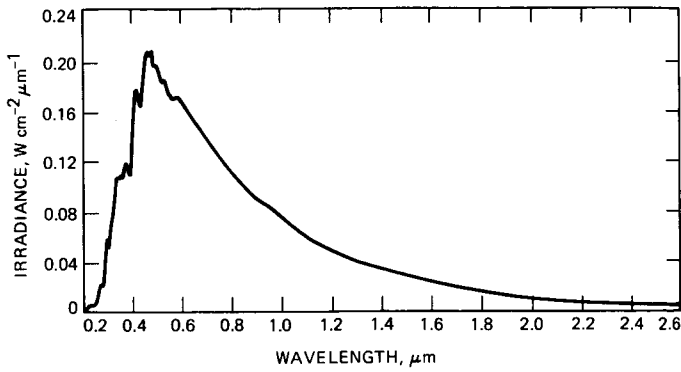


Fig. 1. Solar spectral irradiance (after Ref. 6)

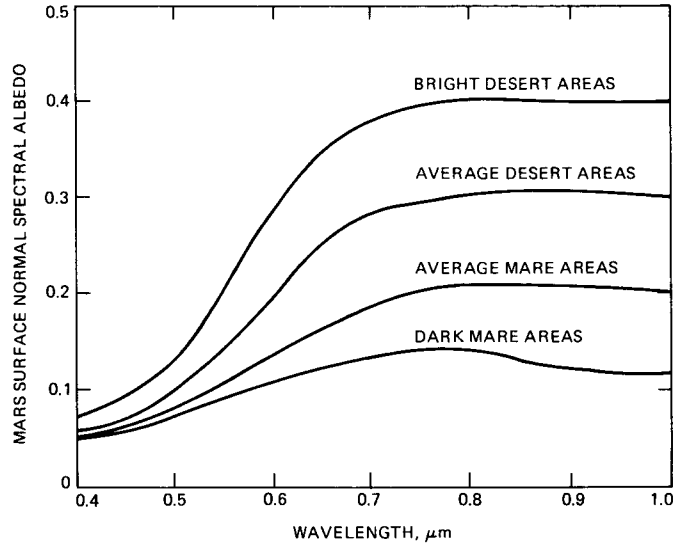


Fig. 3. Estimates of Mars surface normal albedo (after Ref. 7)

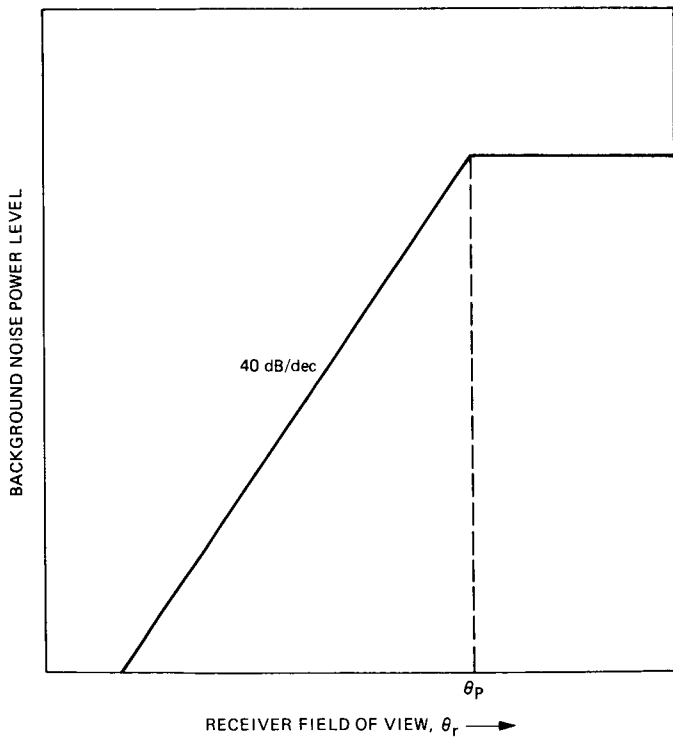


Fig. 2. Background noise power level from a planet vs. receiver field of view

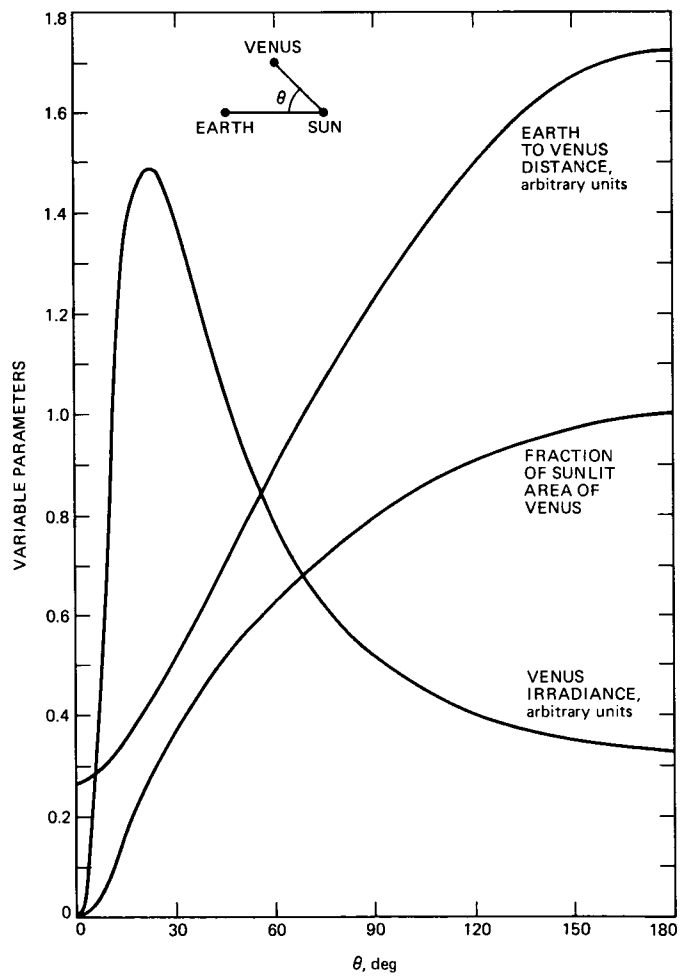


Fig. 4. Dependence of the received background noise from Venus on the Earth-Sun-Venus angle

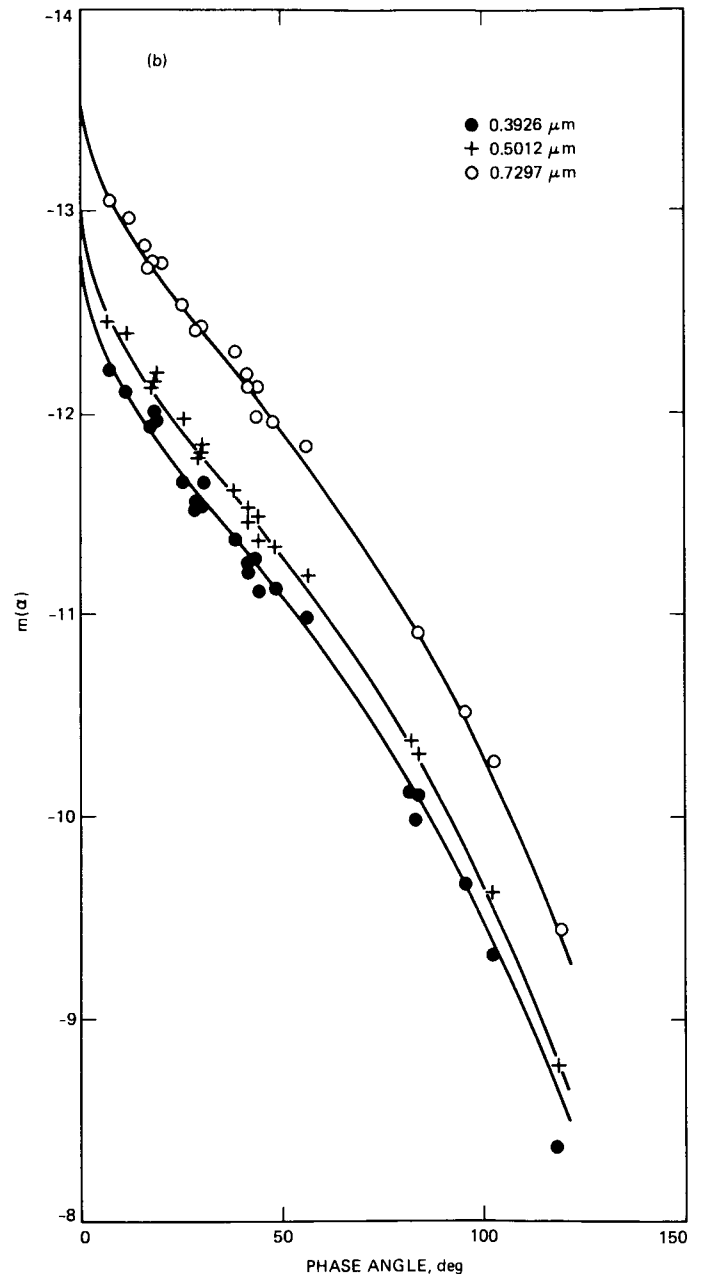
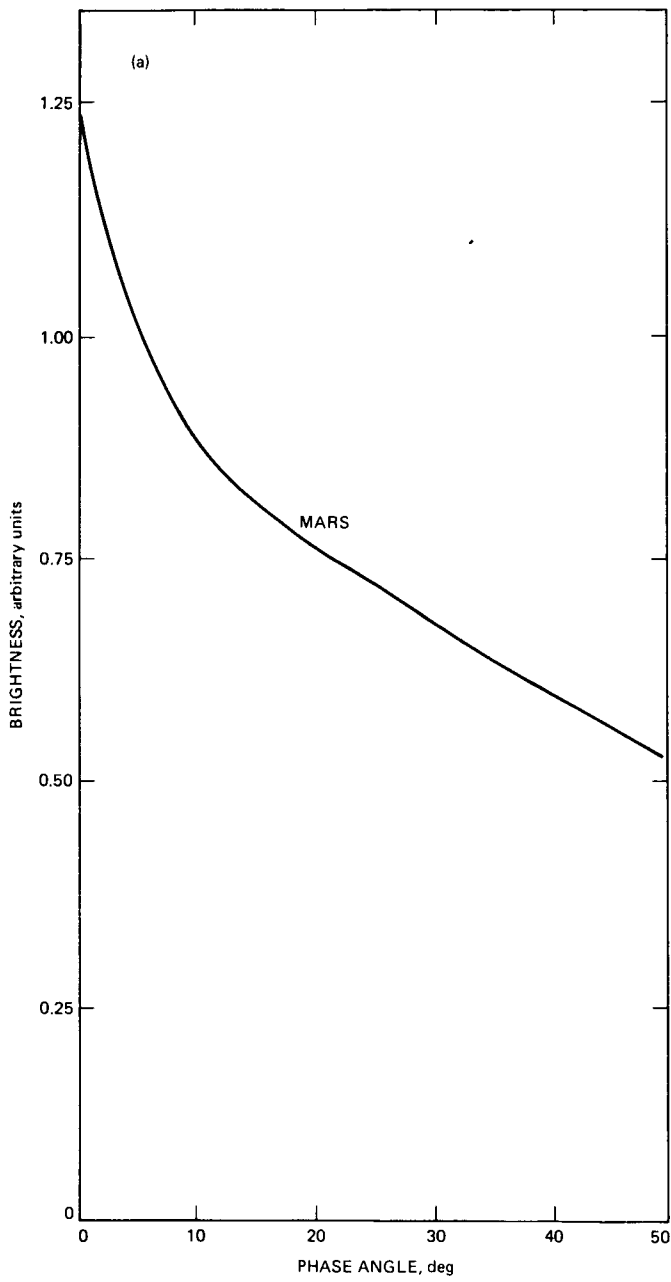


Fig. 5. Phase function (a) for Mars (after Fig. 16.4, Ref. 8) and (b) for Moon (in logarithmic magnitude units, after Fig. 2 in Ref. 9 [III])

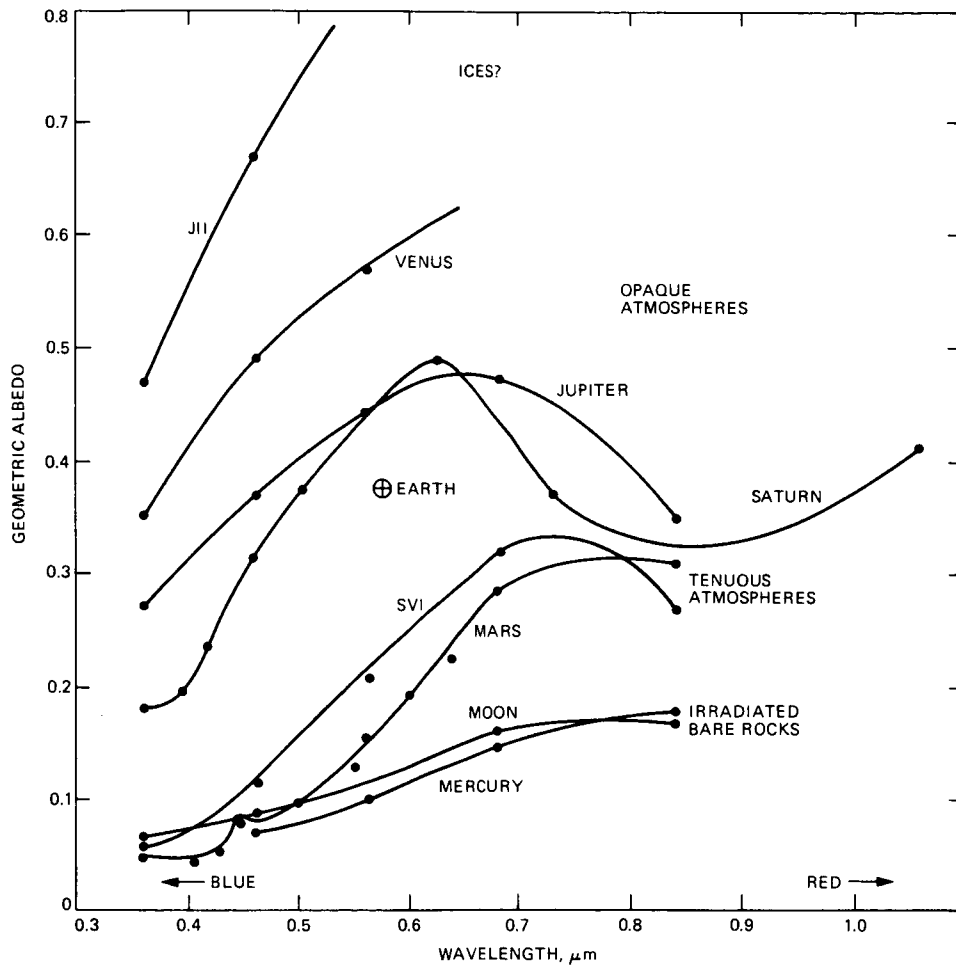


Fig. 6. Geometric albedo (low resolution) wavelength dependence for various planetary bodies (after Fig. 11.7 in Ref. 10 and Table IV in Ref. 13)

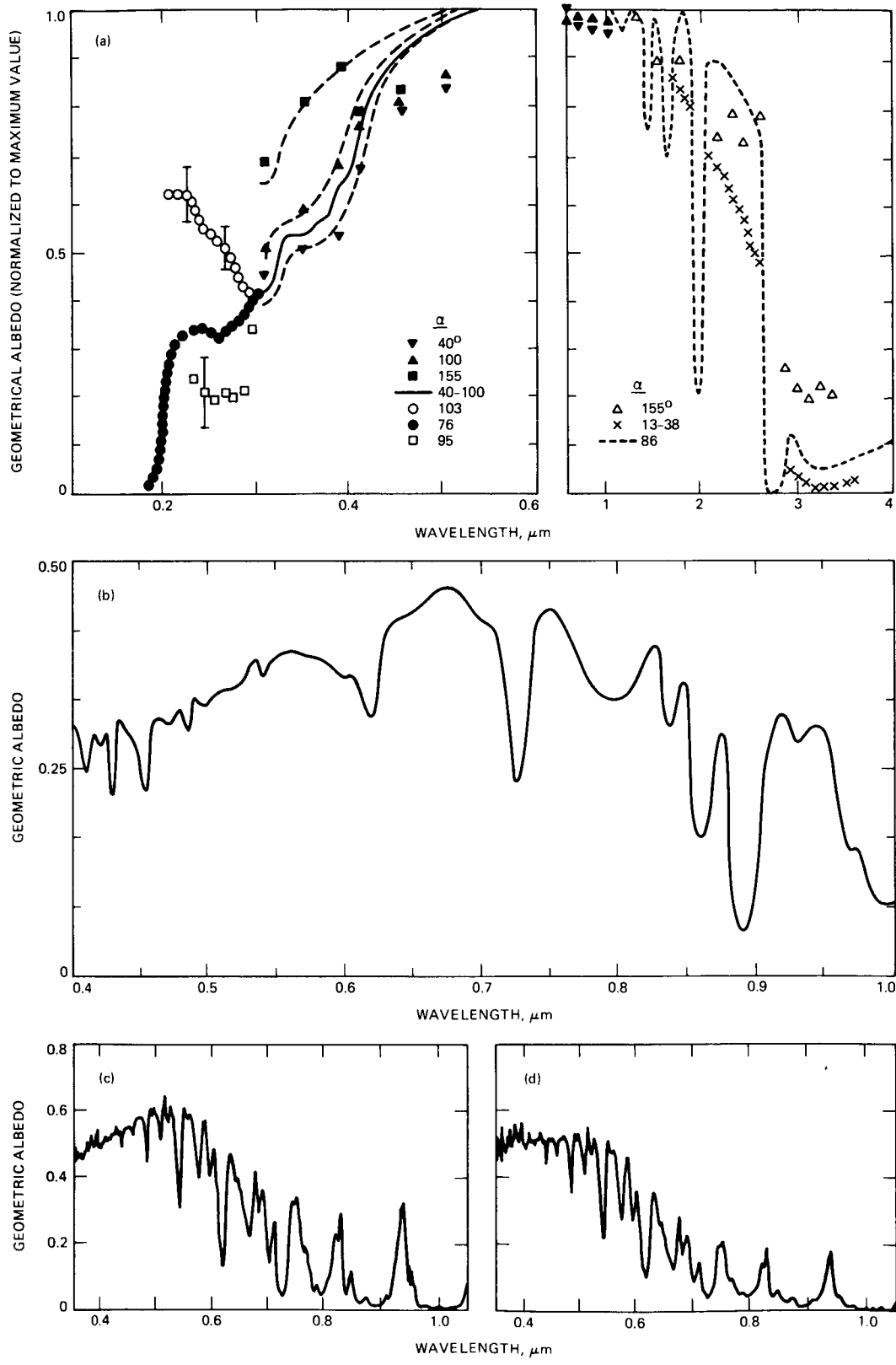


Fig. 7. Detailed geometric albedo for various planets: (a) Venus (after Fig. 1 in Ref. 11); (b) Jupiter (from data in Ref. 12); (c) Uranus (after Fig. 7 in Ref. 14); (d) Neptune (after Fig. 8 in Ref. 14)

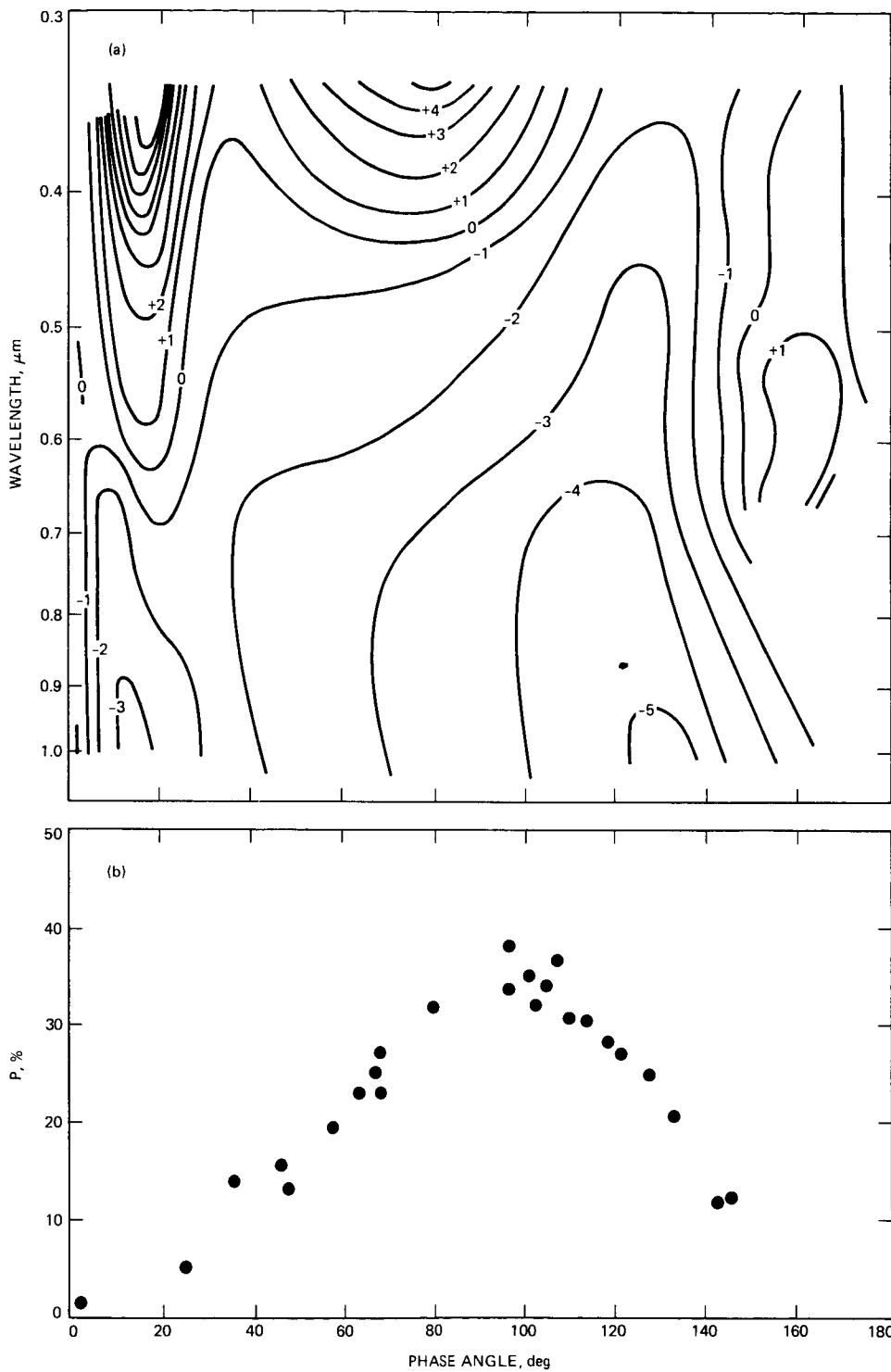


Fig. 8. Polarization: (a) degree of polarization (in percent) of Venus as a function of phase angle and wavelength (after Fig. 16 in Ref. 15) and (b) global earth degree of polarization (after Fig. 24 in Ref. 15)

Appendix A

Phase-Angle Dependence

Consider the sun-planet-earth system shown in Fig. A-1 (for an inner planet in this particular case). The lit angle of the cross sectional disc is $\pi - \alpha$, where α is the phase angle. Choosing θ (planet-sun-earth angle) as the natural coordinate for this problem, it is clearly seen that

$$\pi - \alpha = \theta + \gamma(\theta) \quad (\text{A-1})$$

where $\gamma(\theta)$ is the Sun-Earth-Planet angle, given by

$$\gamma(\theta) = \frac{1}{\sin \theta} \left[\frac{R_{E\odot}}{R_{P\odot}} - \cos \theta \right] \quad (\text{A-2})$$

Simple trigonometric calculations show that the fraction of the lit planetary disc is

$$\sin^2 \frac{\alpha}{2} = \sin^2 \left[\frac{\theta + \gamma(\theta)}{2} \right] \quad (\text{A-3})$$

and that the Earth-Planet distance is given by

$$Z = R_{E\odot} \left[\frac{\sin \theta}{\sin[\theta + \gamma(\theta)]} \right] = R_{P\odot} \frac{\sin \theta}{\sin[\gamma(\theta)]} \quad (\text{A-4})$$

As long as the planet appears as an extended background source, its noise contribution is not affected by the above considerations. However, when the planet is small enough to be considered as a point source, its actual noise is proportional to the ratio of the fractional area lit (Eq. [A-3]) to the distance (Eq. [A-4]). This dependence is strongest for the inner planets, as shown in Fig. 4. For the outer planets, though, the fractional area lit is always close to unity (for Mars the minimum is approximately 87% and the planets from Jupiter and beyond are always more than 99% lit), so the main effect on the noise variation is the Earth-Planet distance.

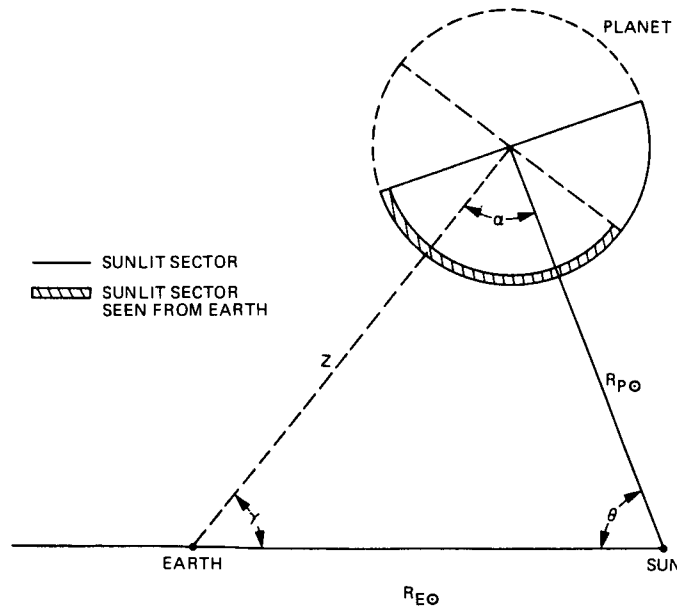


Fig. A-1. Sun-planet-earth system (for inner planet)